RESEARCH ARTICLE

VOLCANICA

Spatial distribution and structural analysis of the Neogene Siroua volcanic field (Moroccan Atlas Mountains)

Mustapha Bouiflane*[α], Nicolas Le Corvec[β], Ahmed Manar[γ], and Riccardo Lanari[δ]

[α]Department of Physique du Globe, Institut Scientifique, University Mohammed V in Rabat, Avenue Ibn Batouta, P.B. 703, 10106 Rabat-Agdal, Morocco.
[β]Independent Researcher, 33200 Bordeaux, France.
[γ]Direction de Géologie, Ministère de la Transition énergétique et du Développement durable, Morocco.
[δ]Institute of Geosciences and Earth Resources, National Research Council – CNR, Florence, Italy.

Abstract

Monogenetic volcanic fields develop worldwide in different geodynamic settings, and understanding their evolution may provide crustal, thermal, and topographical constraints. We focus on the small monogenetic Siroua volcanic field that has formed since the late Miocene along the tectonic lineament separating the High Atlas and the Anti-Atlas Mountains of Morocco, though the evolution of which is still unclear. We investigate the formation and evolution of the Siroua monogenetic field using geostatistical methods that allow us to classify the spatial distribution of vents in their geological contexts. In addition, we use aeromagnetism to obtain information about the tectonic structures underlying the field. Each method is evaluated separately, and then combined to discuss the relationship between the volcanism and the tectonic framework at regional and local scales. Our findings indicate that although vents are broadly randomly distributed, some correlation between volcanic alignments and the structural framework is locally observed. These findings corroborate existing knowledge about the influence of pre-existing structures on the propagation of magmas and on the spatial distribution of volcanic vents within monogenetic volcanic fields.

Keywords: Siroua volcanic field; Spatial distribution; Nearest neighbor; Kernel density; Pre-existing structures; Volcano-tectonic interaction.

Submitted: 2023-10-21 | Accepted: 2024-09-24 | Published: 2024-12-03

Editor: J Farquharson | Typesetter: J Farquharson

1 Introduction

Monogenetic volcanic fields are common volcanic geological features occurring worldwide across all tectonic settings, including extensional settings [e.g. Menzies et al. 1985], subduction zones [e.g. Connor 1987], and intraplate locations [e.g. Cañón-Tapia 2016]. Monogenetic volcanic fields consist of small-volume volcanoes ($\leq$1 km^3), which have erupted through one continuous or many discontinuous small eruptions [e.g. Németh and Kereszturi 2015] fed directly from the deep mantle region [Smith and Németh 2017] by one or a few small-volume magma batches. Some monogenetic fields only host a few volcanoes, while others host hundreds of centers [e.g. Le Corvec et al. 2013b]. The surface expression of monogenetic volcanism exhibits a wide diversity of volcanic morphologies, including lava domes, scoria cones, tuff cones, tuff rings, maar-diatreme volcanoes, small explosion craters, necks, and lava flows [e.g. Connor et al. 2000; Németh 2010; Németh and Kereszturi 2015; Smith and Németh 2017], and the composition can vary from basic to as acidic as rhyolites [e.g. Austin-Erickson et al. 2011]. Monogenetic volcanic fields are still the subject of intense research worldwide to elucidate their geological formation and behavior through time because a considerable number of monogenetic fields are geologically active and some have developed within or near urban areas, e.g. Auckland, New Zealand; Makkah City, Saudi Arabia; Iceland; and Mexico City [Rossi 1996; Agustín-Flores et al. 2011; Bebbington and Cronin 2011; Runge et al. 2014].

Understanding the potential link between monogenetic volcanic fields and tectonic structures may provide crucial constraints for connecting crustal deformation with volcanism. In this sense, we here propose an approach based on the combination of both spatial distribution analyses (i.e. clustering, and spatial distribution of vents) and aeromagnetism to better understand the volcanic feeding systems and the tectonic setting at regional and local scales. We study the Siroua volcanic field, which was active during the Neogene-Quaternary period [Berrahma and Delaloye 1989; Berrahma et al. 1993; Lanari et al. 2023a]. Its relationship with the tectonic evolution of the area is still not clear. Indeed, in the Anti-Atlas, landform analyses indicate late-Miocene uplift [Aït Hssaine and Bridgland 2009; Guimerà et al. 2011] that is coeval with a late Miocene volcanic event, including activity of two volcanic fields: the Siroua in the western, and the Saghro in the eastern (Figure 1) [Berrahma et al. 1993; Guimerà et al. 2011]. Furthermore, the presence of lithospheric tectonic discontinuities mainly the Anti-Atlas Major Fault (AAMF), which is inherited from the Pan-African orogenic events [Choubert 1947] and cross-cutting the Siroua volcanics field [Lanari et al. 2020a] may suggest potential tectonic control in it evolution.

2 Tectonic and volcanic settings

2.1 Tectonic setting

The Atlas Mountains, consisting of the High, Middle, and Anti-Atlas, represent a complex tectonic setting resulting from the Variscan orogenesis, Mesozoic rifting, and Cenozoic compression [Mattauer et al. 1972; Mattauer et al. 1977; Proust et al.

* mustapha.bouiflane@is.um5.ac.ma

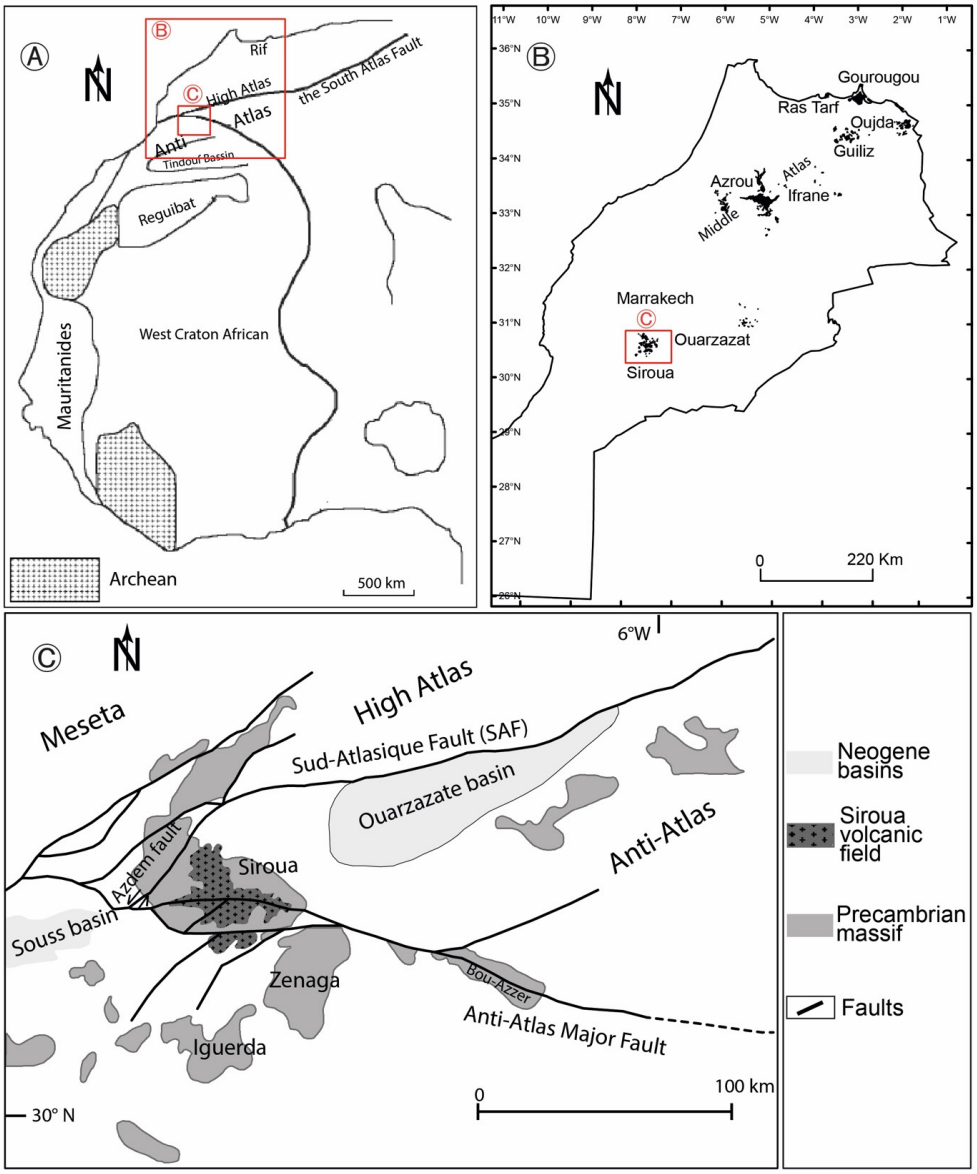

Figure 1: [A] Geological sketch map of the West African Craton, location of the Siroua volcanic field in an area lying between the High-Atlas and the Anti-Atlas Mountains. [B] The three main Neogene-Quaternary volcanic groups from north to south Morocco: 1) the Eastern Rif mountain-belt, featuring the Ras Tarf, Gourougou, Trois Fourches, and Jbel Guilliz volcanic fields; 2) Middle Atlas, including the Ifrane-Azrou volcanic field; 3) Siroua volcanic field, situated between the High Atlas and the Anti-Atlas Mountains. [C] Schematic geological map showing the location of the Siroua volcanic field and its relation to nearby Precambrian inliers, Neogene basins and faults.

1977; Frizon de Lamotte et al. 2000; Ait Brahim et al. 2002] (Figure 1C, Figure 3). Field geological surveys and thermochronological studies indicate that the High Atlas Mountains have experienced a compression phase that began during the late Eocene [Frizon de Lamotte et al. 2009; Leprêtre et al. 2015; 2018; Lanari et al. 2020a; b; 2023b]. The main surge of compression started in the middle to late Miocene (see compilation and reconstruction presented in Lanari et al. [2023b]) and persisted at lower rates until recent times [Arboleya et al. 2008; Tesón and Teixell 2008], with evidence of surface uplift also observed in the surrounding regions [e.g. Clementucci et al. 2023a; b] and volcanism [e.g. Lanari et al. 2023b].

However, in the Anti-Atlas, Miocene deformation is not documented, except for a large E–W Anti-Atlas Major strike-slip fault system cutting the Siroua massif to the south [Lanari et al. 2020a]. In addition, landform analyses indicate late-Miocene uplift [Aït Hssaine and Bridgland 2009; Guimerà et al. 2011] that is coeval with a late Miocene volcanic event, including activity of the Siroua volcanic field.

In the High Atlas, morphological and seismotectonic evidence indicate active Quaternary uplift and deformation [e.g. Meghraoui et al. 1999; Sébrier et al. 2006; Boulton et al. 2014; Pastor et al. 2015], whereas the Quaternary evolution of the Anti-Atlas is still poorly constrained. There, volcanism ceased after 2 Ma [Berrahma and Delaloye 1989; Berrahma et al. 1993],

and morphological features suggest a waning of uplift since ~2 Ma [Lanari et al. 2022].

The Siroua volcanic field is bounded by the following structures: (i) in the north by the E–W trending crustal fault named the "South Atlas Fault," which corresponds to a major strike-slip zone inherited from the Pan-African orogeny; (ii) in the east by the NE–SW striking transform fault of Azdem, which acts as a transfer fault connecting the west segments of the South Atlas Fault with the east segment of the South Atlas Fault, (iii) in the southern part by the E–W trending crustal fault named the "Anti-Atlas Major Fault," which corresponds to a major strike-slip fault zone. The Anti-Atlas Major Fault (AAMF), which is inherited from the Pan-African orogenic events [Choubert 1947], runs roughly E–W, and subdivides the Anti-Atlas belt into two distinct domains [Ennih and Liégeois 2001], (1) the western and central Anti-Atlas, SW and along the AAMF; and (2) the eastern Anti-Atlas, situated NE of the AAMF to the South Atlas Fault (SAF) (Figure 1).

2.2 Volcanic setting

Jurassic, Paleogene, and Neogene/Pleistocene volcanic products are widespread throughout northwestern Africa and southern Spain [e.g. Turner et al. 1999; Duggen et al. 2009; Casalini et al. 2022]. However, only the late Miocene volcanism occurs together with the orogenic evolution of the High- and Middle-Atlas [e.g. Lanari et al. 2023a]. In Morocco, from north to south, we can identify: (i) the Eastern Rif mountain belt, featuring the Ras Tarf, Gourougou, Trois Fourches, and Jbel Guilliz volcanoes [Hernandez and Bellon 1985; El Bakkali 1995; El Bakkali et al. 1998]; (ii) the Middle Atlas volcanic field, comprising the largest and youngest basaltic volcanic province in Morocco [Choubert et al. 1968; Bellon 1976; Harmand and Cantagrel 1984; Moukadiri and Pin 1998; El Azzouzi et al. 1999; Amine et al. 2019; Benamrane et al. 2022; 2023]; and (iii) the Siroua and Saghro volcanic fields in an area lying between the High-Atlas and the Anti-Atlas Mountains (Figure 1A, 1B) [Rachdi et al. 1985; Berrahma and Delaloye 1989; Berrahma et al. 1993; Berrahma 1995].

The Siroua volcanic field, the focus of our study, covers an area of approximately 600 km^2 and directly overlies the Precambrian basement (Figure 1A), which is composed of an assemblage of plutonic and metamorphic rocks. According to K-Ar dating, Siroua volcanism occurred from the Late Miocene to the Early Pliocene (10.8 to 2.7 Ma [Berrahma et al. 1993]). New K/Ar ages on mafic lavas yield ages between 8.6 and 2.4 Ma [Lanari et al. 2023a], which correspond well with the range of ages previously found for the Siroua and Saghro volcanic fields [Berrahma and Delaloye 1989; Berrahma et al. 1993]. The Siroua volcanic field consists predominantly of tuffs and lavas, the former being more abundant, with predominant air-fall tuffs [Berrahma and Delaloye 1989]. The tuffs are often altered and deposited directly on the Precambrian substratum. The volcanic suite is characterized mostly by hyperalkaline rocks and a few basic rocks, consisting of nepheline-bearing trachyte, quartz trachyte, comendite, phonolite, mugearite, benmoreite, and hawaiite. Ignimbrites also occur but only appear during the latest stage of volcanic activity [Berrahma 1982]. Dykes of trachytes and rhyolites associated with pyroclastics and spectacular phonolitic domes and necks are found in the center and northern part of the Siroua volcanic field (Figure 2), whereas the southern part consists of trachytic lava flows.

3 Methods

3.1 Spatial distribution analysis of volcanic edifices

Spatial distribution analysis is an important tool for studying volcanic fields. Understanding the spatial distribution of volcanic activity within a volcanic field can provide insights into the underlying volcanic plumbing system as well as the crustal mechanical layering and help to understand the factors that control the temporal evolution of monogenetic volcanic fields [e.g. Mazzarini 2003; 2007; Mazzarini et al. 2010; Le Corvec et al. 2013a; b; Muirhead et al. 2016a; b].

There are several statistical methods to analyze the spatial distribution of volcanic fields. These involve calculating various measures of spatial clustering or dispersion and the spatial density of volcanic vents within a volcanic field. In this work, we adopted a combination of Poisson nearest-neighbor analysis and kernel density estimation to get quantifiable results of the spatial analysis in the Siroua volcanic field.

3.1.1 *Poisson nearest neighbor analysis*

Poisson nearest neighbor analysis is a statistical test (R) commonly used in the study of the spatial distribution of volcanic constructs in a volcanic field. This method can help to determine whether volcanic constructs are randomly distributed throughout the field or whether they tend to cluster in certain areas [e.g. Connor and Hill 1995; Condit and Connor 1996; Le Corvec et al. 2013b]. We used the `Geological Image Analysis Software` (`GIAS`*) developed by Beggan and Hamilton [2010] to evaluate the spatial distribution of volcanic centers in each volcanic field, compared to that expected for a Poisson nearest-neighbor statistical model [Clark and Evans 1954]. The `GIAS` inputs are in the form of a two-column table of geographic coordinates of volcanic centers (i.e. point features) directly extracted from the geological map sheet. The main nearest neighbor distances are determined both for the observed population (R_o) and expected distributions in a population (R_e), then their mean distances are calculated to obtain R_o and R_e, respectively [Baloga et al. 2007]. `GIAS` calculates the population density using a convex hull generated by connecting the outermost points of the population [Hamilton et al. 2010; Le Corvec et al. 2013b], divided by the number of volcanoes per volcanic field. `GIAS` outputs a histogram of the mean nearest neighbor distances and four different graphs, plotting: (i) the volcanic edifices and the convex boundary hull of the field; (ii) an R statistical value and a C statistical value resulting from the nearest neighbor analysis, plotted with a confidence interval of 2σ; and (iii) the skewness versus kurtosis.

R compares the spatial distribution of the natural system with the Poisson model, while C assesses the significance of this comparison. Hamilton et al. [2010] described different scenarios depending on the relationship between the R and C values and their respective thresholds of significance:

*www.geoanalysis.org

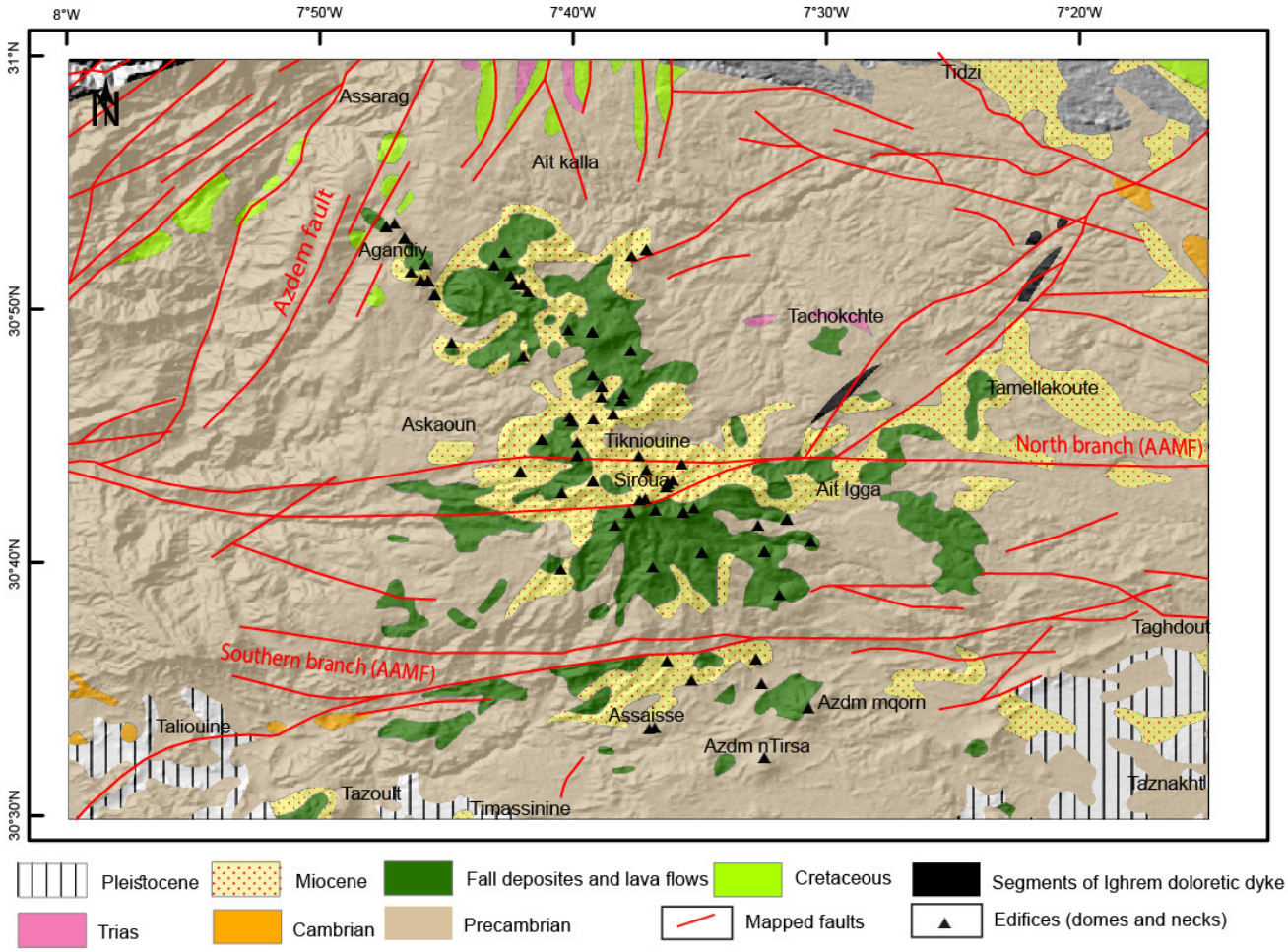

Figure 2: Geological map of the study area. Shaded relief map displaying the main faults, the distribution of volcanic edifices (black triangles), and the deposits of the Siroua volcanic field. AAMF denotes the Anti-Atlas Major Fault. Faults are compiled from the Taliouine geological map-sheet at a scale of 1:100,000 which also yielded the volcano coordinates.

Figure 3: Volcanic edifices in the central part of the Siroua volcanic field (Siroua area). The summit of the highest volcano, Adrar n'Siroua, is 3,304 m above sea level.

1. If R and C fall within ±2σ of the significance level of their expected values, the observed distribution is consistent with the Poisson model (i.e. randomly scattered).

2. If C falls outside the ±2σ of the significance level, and R is larger than +2σ, the Poisson model is rejected, and the observed distribution is dispersed relative to the Poisson distribution.

3. If C falls outside the ±2σ of the significance level, and R is less than −2σ, the Poisson model is rejected, and the observed distribution is clustered relative to the Poisson distribution.

4. If C falls within ±2σ of the significance level, and R falls outside ±2σ, the spatial distribution shows equivocal significance, and the result is not interpretable.

3.1.2 *The Kernel density estimation*

Kernel density estimation is a commonly used statistical method in a wide range of fields, including volcanology, to evaluate the spatial density of volcano locations. This method can provide insights into the behavior of volcanic systems [e.g. Connor and Hill 1995; Lutz and Gutmann 1995; Connor et al. 2000; Martin et al. 2004]. Kernel density estimation is a non-parametric method that estimates the probability density function of random variables [Silverman 1986]. It estimates the value of the target variable per unit area from point data (i.e. volcanic vent coordinates), fitting a probability density function to each point.

Let $(x_1, x_2, ..., x_N)$ be independent and identically distributed random variables from some distribution with an unknown probability density function $(\widehat{f})$. In the statistical literature, it is common to read that a nonparametric estimator of the probability density functions can be obtained by evaluating:

$$\widehat{f}(x) = \frac{1}{Nh} + \sum_{i=1}^{N} K\left(\frac{x - X_i}{h}\right) \quad (1)$$

where $K()$ is the kernel (a symmetric probability density function), X_i, represents one of the N observations, and $h > 0$ is a smoothing parameter (known as the bandwidth or search radius). The commonly used Kernel functions are Gaussian, uniform, and triangular. However, the Gaussian kernel is often used because it has convenient mathematical properties compared with the other kernels [Wand and Jones 1994], with a small efficiency loss. The spatial distribution of the volcanic edifice density in a volcanic field is computed by applying a two-dimensional, symmetric Gaussian kernel density function [e.g. Connor and Connor 2009; Kiyosugi et al. 2012; Bartolini et al. 2013; Cañón-Tapia 2016; Morfulis et al. 2020; Cañón-Tapia 2022].

3.2 Alignment analysis of volcanic edifices

Several authors describe cases where the alignment of edifices within volcanic fields seems to be influenced by both regional and local stress fields and pre-existing structures [e.g. Le Corvec et al. 2013b, and references therein]. Some studies on volcanic fields describe cases where volcanic edifices appear to be aligned along pre-existing faults [Lesti et al. 2008; Boyce 2013; Jordan et al. 2013; Blaikie et al. 2014; Van Otterloo et al. 2014; Cas et al. 2016]. Moreover, according to Cebriá et al. [2011], the closer the vents are to each other, the higher the probability that they are fed by the same fissure and, consequently, that they are aligned along a fracture. This would imply that quantifying azimuth trends of faults underlying a volcanic field is necessary for determining whether a spatial relationship exists between the alignment of edifices and fault trends.

3.3 Aeromagnetism

Aeromagnetism is a geophysical exploration technique deployed for mineral exploration and has been used with success to complement geological data [e.g. Milligan and Gunn 1997; Isles and Rankin 2013]. Furthermore, the application of aeromagnetic surveys to map tectonic structures has increased with the development of high-resolution surveys and filtering techniques [e.g. Nabighian et al. 2005]. Among other results, magnetic grid anomalies obtained after applying various filters to a recorded geomagnetic field offer the possibility to produce azimuths of faults underlying volcanic fields and sedimentary basins.

3.3.1 *Geomagnetic fault detection*

Faults or fault segments can often be simplified as planar geological features. They are commonly observed at the surface, buried near the surface (i.e. covered mostly by younger sediments and lava flows), or they affect basement rocks more deeply, making them difficult to detect by geological observation alone. A detailed analysis of magnetic data can yield important insights into the structural framework of a volcanic field, and several studies have demonstrated that high-resolution aeromagnetic data allows for the improvement of structural models [e.g. Grauch 2001; Grauch et al. 2006; Grauch and Hudson 2007]. Based on the literature, faults are expressed as linear contrasts (i.e. magnetic lineaments) [e.g. Finn and Morgan 2002]. However, the recognition of faults in aeromagnetic data can be challenging because most faults do not have a direct magnetic signature [Isles and Rankin 2013]. In this case, various typical magnetic signatures of faults can assist the interpreter in providing evidence that the linear anomalies are aeromagnetic expressions of faults, such as: (i) the dislocation of lateral continuity of a magnetic lineament, (ii) apparent displacement of a magnetic lithological boundary, (iii) traces where the presumed fault disrupts the continuous magnetic lineament, causing significant left-lateral or right-lateral offsets, and (iv) the consistent correspondence to mapped faults. Considering the geological context of our study, we interpret magnetic lineaments that may be associated with faults with caution, since similar lineaments may also originate from artifacts due to non-uniform terrain clearance and topographic effects [e.g. Grauch 2001; Grauch et al. 2006; Grauch and Hudson 2007].

To distinguish magnetic signatures corresponding to faults from the rest of the magnetic anomalies, a set of transformations are applied step by step to the magnetic data. These

transformations are a set of mathematical filters offered by the OASIS Montaj software*. In the following, we will present the enhanced processing steps for fault identification.

3.3.2 *Enhanced processing steps*

Reduction to the pole transformation. The reduction to the pole transformation is a technique that minimizes the polarity effects of a magnetic anomaly [Baranov 1957; Baranov and Naudy 1964; Blakely 1995]. These polarity effects manifest as a shift of the main anomaly away from the center of the magnetic causative source, due to the magnetic inclination and declination angles at the location of the measurement. The reduction to the pole transformation positions anomalies directly above their causative geological bodies, thereby facilitating the interpretation of aeromagnetic anomalies and their comparison with geological data.

The reduction to the pole of aeromagnetic data was computed from the residual magnetic anomaly grid by considering the magnetic field inclination and declination angles at the location and the time they were conducted.

Vertical derivative transformations. To improve the magnetic signature of faults, a set of magnetic derivative transformations, preferably applied to the reduction to the pole anomaly grid, is used. These transformations include band-pass filters, which accentuate the magnetic signal and reveal linear anomalies over geological contacts such as faults, edges of intrusions, and dikes [Cordell and Grauch 1985]. They are often referred to as "Edge detectors" filters [Blakely and Simpson 1986]. Various derivatives (or gradients) can be applied in terms of the directions of the derivative (x, y, and z) and orders of the derivative (commonly first order). The first-order vertical derivative of the magnetic field intensity is given by [Evjen 1936]:

$$\mathrm{VDR}_{(z)} = \frac{\partial F}{\partial z} \tag{2}$$

where $\frac{\partial F}{\partial z}$ represents the vertical (z) derivatives of the magnetic field intensity (F).

Tilt derivative transformations. The tilt derivative is a geometrical function of the vertical $\left(\frac{\partial F}{\partial z}\right)$ and horizontal $\left(\frac{\partial F}{\partial x}\right)$; $\left(\frac{\partial F}{\partial y}\right)$ derivatives of the magnetic field intensity (F). The tilt derivative is in fact an angle parameter with values ranging between ($\pi/2$ and $\pi/2$), the zero contours locating close to the source–body contact. The tilt derivative as applied equalizes the total field amplitudes and thus emphasizes structural features [Miller and Singh 1994; Verduzco et al. 2004]. This derivative is particularly useful for detecting subtle magnetic lineaments that are not so evident in the original data and provides greater confidence in mapping faults and shear zones [Lahti and Karinen 2010; Fairhead et al. 2011]. The tilt derivative is given by:

$$\mathrm{TDR} = \theta = \arctan\left(\frac{\frac{\partial F}{\partial z}}{\sqrt{\left(\frac{\partial F}{\partial x}\right)^2 + \left(\frac{\partial F}{\partial y}\right)^2}}\right) \tag{3}$$

where $\left(\frac{\partial F}{\partial x}\right)$ and $\left(\frac{\partial F}{\partial y}\right)$ are the horizontal (x, y) derivatives, and $\left(\frac{\partial F}{\partial z}\right)$ is the vertical (z) derivative of the magnetic field intensity (F).

All derivative filters were computed after the reduction to the pole transformation. The grid was further upward continued by a distance of 150 m in order to diminish the high-frequency noise associated with the leveling effects.

4 Database

4.1 Spatial distribution data

We created a spatial database using point features (i.e. volcanic edifices coordinates) by identifying the volcanic edifices through both the geological map-sheet of Taliouine 1:100,000 covering the entire Siroua volcanic field† and Google Earth. We visually identified a total of 65 individual volcanic edifices, mostly classified as lava domes and necks (Figure 3).

4.2 Structural data

The faults are compiled from the geological map-sheet of Taliouine 1:100,000 covering the entire area (Figure 3) and inferred faults derived from aeromagnetic maps (Figure 7).

4.3 Aeromagnetic data

The helicopter-borne geophysical survey was carried out in 1998 by Fugro Airborne Surveys Inc. for the Ministry of Energy and Mines, Morocco‡, covering most of the Anti-Atlas domain as well as the Siroua volcanic field and several areas in Morocco for mineral exploration objectives§. The airborne geophysical surveys are operated using multisensor equipment simultaneously, including, the DIGHEM® multi-frequency electromagnetic system (DIG: digital, H: helicopter-borne, EM: electromagnetic), supplemented by a 256-channel Gamma-Ray spectrometry and scalar magnetic measurements. The magnetic measurements were collected with a Scintrex CS-2 Cesium vapor magnetometer (sensitivity of 0.01 nT). The magnetometer samples 10 times a second, resulting in a magnetic measurement sampling interval between 2 and 3 m along flight lines. The survey was flown at a low nominal flight altitude of 30 meters (30 m draped above the topography), with 500 m spacing between the traverse lines and 5000 m spacing between the tie lines flown perpendicular to the traverse lines. The magnetic datasets were interpolated onto a square grid with a cell size of 125 m using the minimum curvature method. The airborne magnetic data were obtained in the form of a residual magnetic anomaly after subtracting the International Geomagnetic Reference Field (IGRF epoch) values from the total magnetic intensity data.

*https://www.seequent.com/products-solutions/geosoft-oasis-montaj/

†source: www.cartesgeoscientifiques.mem.gov.ma

‡www.mem.gov.ma

§source: www.cartesgeoscientifiques.mem.gov.ma

5 Results

5.1 Spatial analysis results

5.1.1 *Poisson nearest neighbor analysis*

The result of the Poisson nearest-neighbor analysis (Figure 4 and Table 1) shows that the spatial distribution of the volcanic edifices within the Siroua volcanic field is random and similar to the Poisson distribution.

Table 1: Parameters and results from Poisson nearest neighbor analysis.

Parameters	Results
Total # of volcanic edifices (N)	65
Area convex hull (m^2)	5.51×10^8
Density (ρo) (# edifices m^{-2})	1.03×10^{-7}
Minimum NN Distance (m)	334.67
Maximum NN Distance (m)	6059.92
Mean distance NN (Ro) (m)	1499
Expected Poisson distribution (Re) (m)	1554
R	0.965
Ideal *R*	1.0601
R positive thresholds at 2σ	1.2169
R negative thresholds at 2σ	0.9033
Distribution implication	Random
C	−0.506
Ideal *C*	0.8722
C positive thresholds at 2σ	3.1394
C negative thresholds at 2σ	−1.395
Model fit implication	Significant

5.1.2 *Kernel density estimation result*

The vent density distribution map, produced by applying the kernel density estimation (Figure 5 and Figure 8), clearly shows four clusters: (a) two clusters (1 and 2) in the center of the Siroua volcanic field, forming ellipses with long axes trending NE–SW; (b) in the Agandy region (north of the Siroua volcanic field), two clusters 3 and 4 consist of volcanic edifices inside ellipses with long axes trending NNW–SSE; (c) in contrast, the southern portions of the Siroua volcanic field present lower densities and a sparser distribution.

5.2 Interpretation of magnetic anomalies

The residual magnetic anomaly map of the study area (Figure 6A) shows a wide variation in magnetic intensity (from −1394.72 to +1140.64 nT) and enables the identification of several types of anomalies reflecting the geological formations representing different ages of intrusive and extrusive rocks. The residual magnetic anomaly grid was enhanced by applying a reduction to the pole transformation to ascertain the correlation between magnetic anomalies and geological formations. The reduction to the pole map (Figure 6B) revealed a relatively strong magnetic anomaly (3.7 to +1140.64 nT) could be deciphered toward the northern and northeastern parts of the study area, which may be caused by the high susceptibility of Precambrian basement rocks of the Siroua massif [Hodel et al. 2020], and a weaker magnetic anomaly (from −8.2 to −1394.72 nT) towards the southern part, which may reflect a possible transition zone adjacent to the Anti-Atlas Major crustal fault systems. The first-order vertical derivative map (Figure 6C) and tilt derivative map (Figure 6D), obtained after the filtering process, were found to be more informative about the shallow surface features and resulted in a better representation of near-surface features (such as faults).

5.3 Identification of faults from geomagnetism

Figure 6C displays the first-order vertical derivative of the reduction to the pole magnetic field, upward-continued to 150 m, and Figure 6D is the map of the tilt derivative of the reduction to the pole magnetic field, also upward-continued to 150 m. Both the first-order vertical derivative and tilt derivative filters emphasize short-wavelength features and enhance shallow crosscutting or overprinting structures, such as networks of faults and segments of dykes. Magnetic trends of various directions were delineated (Figure 6C), and both positive and negative lineaments were found associated with mapped and unmapped tectonic structures. The positive magnetic lineaments are associated with mapped and covered segments of the Ighrem doleritic dyke. Based on the magnetic structural identification procedure (as explained above), possible fault locations were manually traced along the center of prominent magnetic lineaments on the derivative magnetic maps (i.e. tilt derivative and first-order vertical derivative) and were digitized as polyline shapefiles. The structural pattern, established from inferred faults, is presented in Figure 7.

6 Discussion

6.1 Spatial distribution pattern

Sixty-five volcanic edifices are distributed over 600 km^2 within the study area. A large number of well-exposed monogenetic edifices are still preserved and provide an excellent opportunity to study the geological processes involved in their formation. Two geostatistical methods have been used to scrutinize the distribution of volcanic edifices. Poisson nearest-neighbor analysis indicates that, independently from the tectonic setting, the spatial distribution is consistent with a random Poisson distribution. Morfulis et al. [2020] suggest two styles for monogenetic volcanic fields: (i) fields dominated by magmatic activity, with a clustered pattern and (ii) fields dominated by tectonics, with a random and Poisson distribution pattern. However, in the Siroua volcanic field, although the overall distribution appears "random" and consistent with a Poisson distribution, we applied Kernel density estimation to further investigate the spatial density in zones of distributed volcanism. This method revealed clusters of volcanic edifices over a range of scales, which are not immediately obvious in the broader random pattern. The detected clustering, quantitatively identified through this statistical approach rather than by mere visual inspection, might provide insights into the underlying plumbing system of the volcanic field, the possible relationship with tectonic structures and the local stress regime during the volcanism [e.g. Le Corvec et al. 2013b; Mazzarini and Isola 2021].A similar situation has been reported at other small subsets of monogenetic volcanic fields (e.g. Auckland,

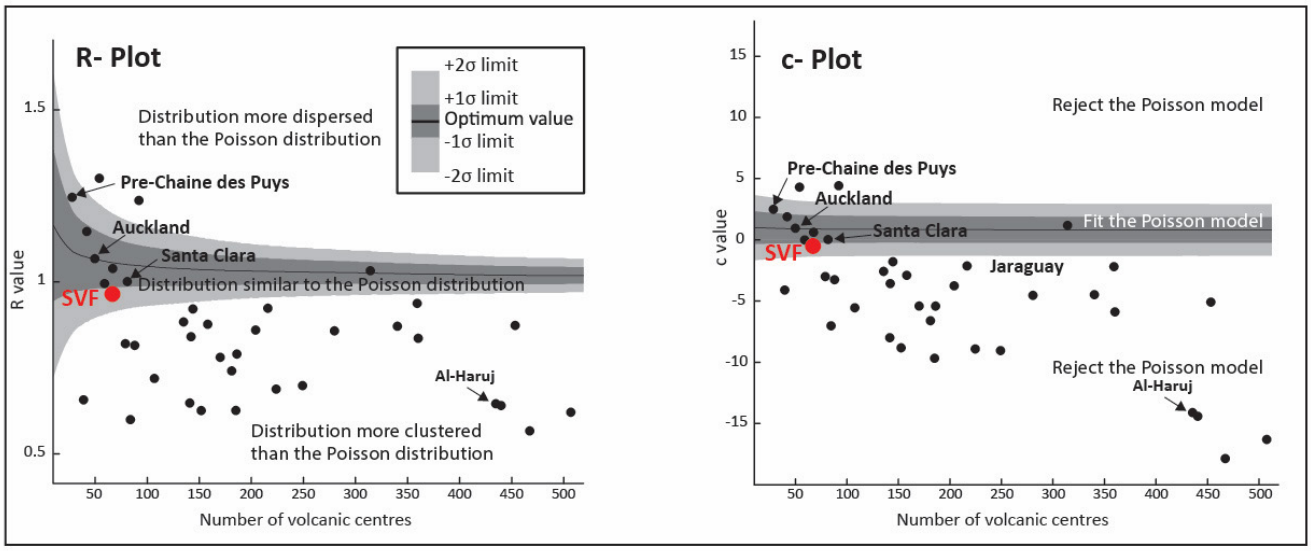

Figure 4: *R*-Plot and *C*-Plot illustrating the *R*-values and *C*-statistics against the number of volcanic centers. The Siroua volcanic field (SVF, indicated by a red dot) is compared with 37 monogenetic volcanic fields studied worldwide [Le Corvec et al. 2013b]. The SVF aligns with a random spatial distribution according to the Poisson model.

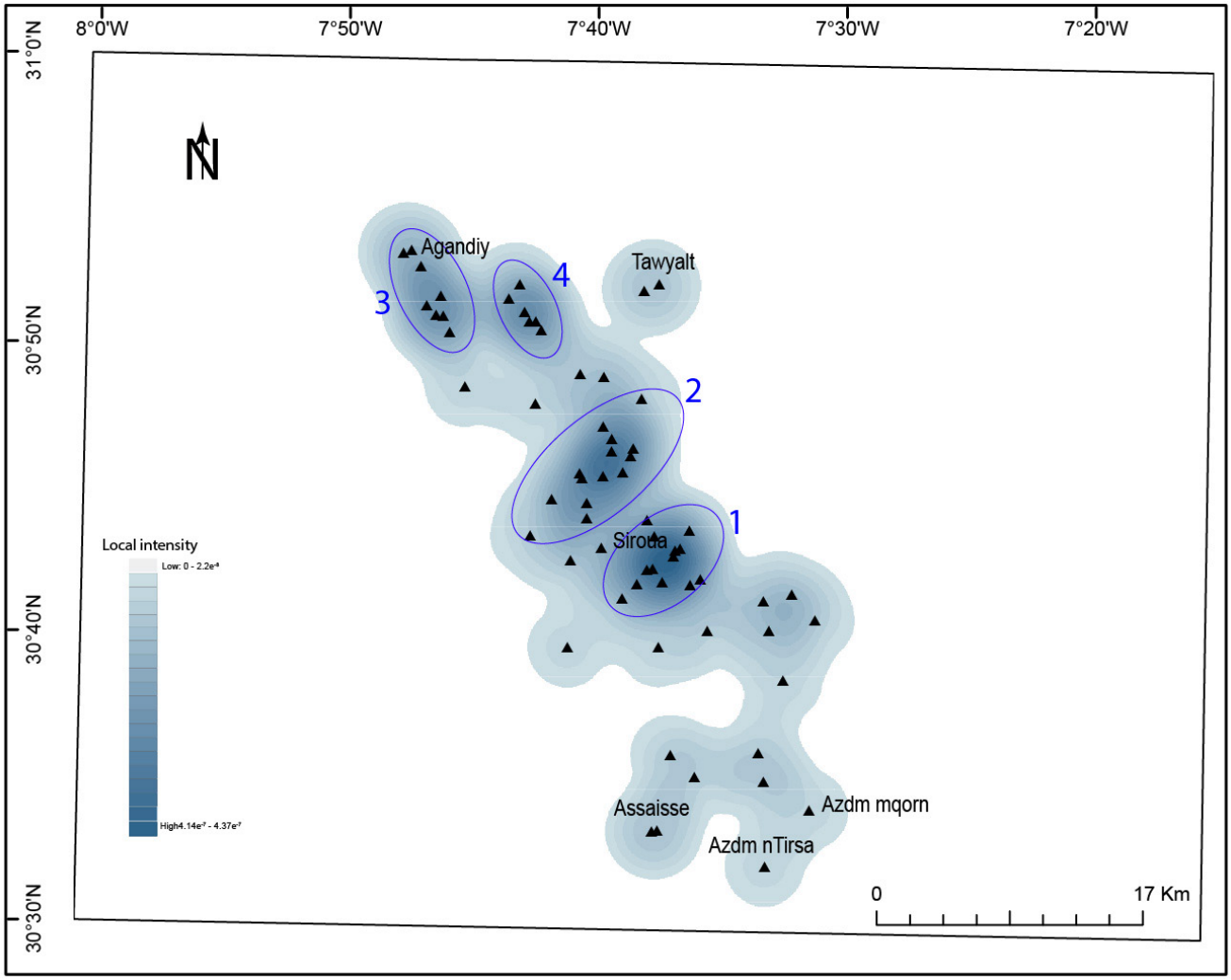

Figure 5: Vent density distribution map derived from Gaussian Kernel analysis (depicted by grey contoured density levels) overlaid with volcanic edifices (black triangles). Agglomerative hierarchical clustering reveals four clusters (blue ellipses).

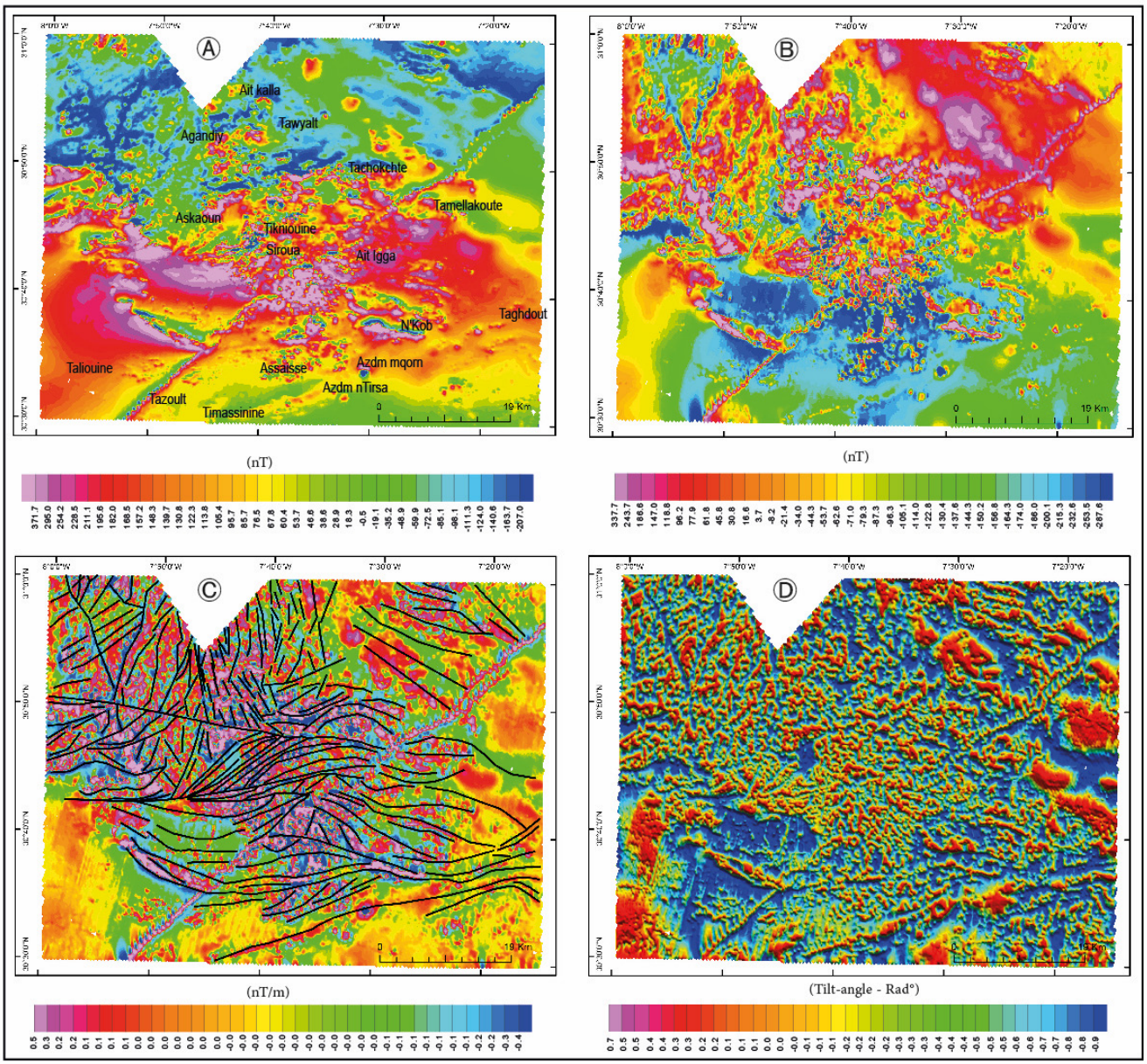

Figure 6: Magnetic anomaly maps of the study area: [A] Residual magnetic field, [B] Reduction to the pole map, [C] Vertical derivative map with traced inferred faults, and [D] Tilt angle map with shaded relief effect.

South Auckland, East Eifel, Pre-Chaîne des Puys, Snake River North Volcanic Fields), which often display random to uniform distributions [Spörli and Eastwood 1997; Le Corvec et al. 2013b].

6.2 Tectonic structures

The azimuths of the inferred fault strikes (Figure 7) indicate that the Siroua area overlies multiple tectonic structures. In the southern portion of the volcanic field, ESE and minor ENE and E–W trends, compatible with the Anti-Atlas Major strike-slip fault, are predominant. Moreover, we observe that some fault segments disrupt the continuous magnetic lineament of the Ighrem doleritic dyke, causing significant left-lateral and right-lateral offsets. Such kinematics, indicating an E–W fault wrench system, are consistent with both the Mesozoic left-lateral rift phase [Mattauer et al. 1972; Mattauer et al. 1977; Proust et al. 1977] and the most recent right-lateral transpressive phase [e.g. Lanari et al. 2020a]. In the central part of the field (Siroua village), we identify a well-developed NE–SW trend nearly parallel to the NE–SW Ighrem dyke. Such a direction is consistent with an overall dextral sigmoidal shape caused by an oblique tectonic direction of compression oriented NW–SE, which characterizes the entire Atlas system at the orogenic scale [Soumaya et al. 2018]. However, an additional minor family of NW–SE faults is inferred between Tachokchout and Tizi villages. In the northern portion of the Siroua volcanic field, we can infer an overall pattern of criss-crossing fault zones with NE–SW trending faults that may be coupled with the NE–SW Azdem transform fault. At the northern border of the field, N–S magnetic lineaments may

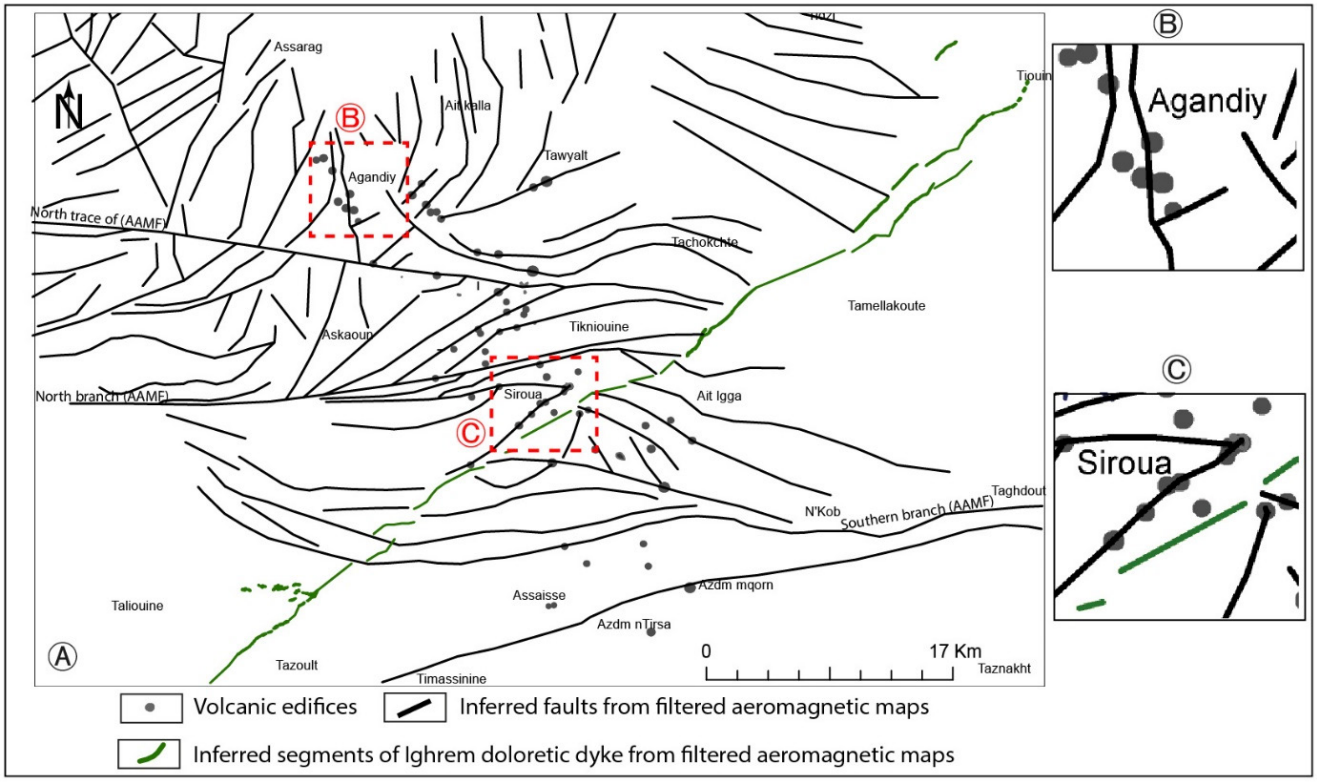

Figure 7: [A] Structural map showing inferred faults (black lines) and the distribution of monogenetic edifices (black dots). Note the N and NW striking faults in the Agandiy area. Insets [B] and [C] provide detailed views of the Agandiy and Siroua areas, respectively, highlighting the relationship between fault patterns and volcanic distribution.

be attributed to the mapped forced folds and reverse faults [Emran and Medina 2016].

6.3 Clustering and volcanic alignments

The Kernel density estimation map (Figure 8) provides a clear image of four clusters: two in the center of the field and two in the northern part of the Siroua volcanic field. The clusters map is then superimposed on the structural pattern established from the inferred faults (Figure 8). The directions of the faults within each cluster were plotted in a rose diagram using `GEOrient` software [Holcombe 2010]. The observed orientation of both faults and the azimuth of the major axis of the ellipse is compared in Table 2.

Table 2: The comparison between the azimuth of the major axis of the ellipse for each cluster and faults orientation inside clusters.

Cluster	Number of volcanic edifices	Azimuth of the major axis of the ellipse (°)	Azimuth of inferred faults (°)
1	12	N49	N45
2	13	N49	N41
3	8	N160	N175
4	6	N157	N135

We observe two preferred orientations: in the central part of the field, both faults and the azimuth of the major axes of the ellipses of clusters 1 and 2 tend to be aligned along an N45° direction. This orientation may be related to the influence of the well-developed ENE–WSW and E–W trends predominantly attributed to the Anti-Atlas Major strike-slip fault that cuts through the Siroua volcanic field. In contrast, in the northern part of the area, both the inferred faults and the azimuth of the major axes of the ellipses of clusters 3 and 4 tend to be aligned along an N165° direction.

The difference in alignment orientation between the central and northern parts of the Siroua volcanic field could be explained by the influence of the structures and the local stress regime at the time of volcanic activity. In terms of magma emitted in the field, the Kernel density estimation maps (Figure 5 and Figure 8) show that the greatest density of volcanic edifices is in the central part of the Siroua volcanic field, around Siroua, with a density of 36 edifices compared to 21 in the northern part, and the lowest density of volcanic vents, with only 8 edifices, is found in the southern part. This non-clustered distribution and fewer numbers of edifices in the southern portion of the Siroua volcanic field could be explained by a low concentration of tectonic structures favoring the magma ascent. Additionally, age differences among the volcanoes within these clusters might also influence the observed spatial distribution. The presence of younger or older volcanic features could correlate with phases of tectonic activity, providing further insights into the clustering pattern.

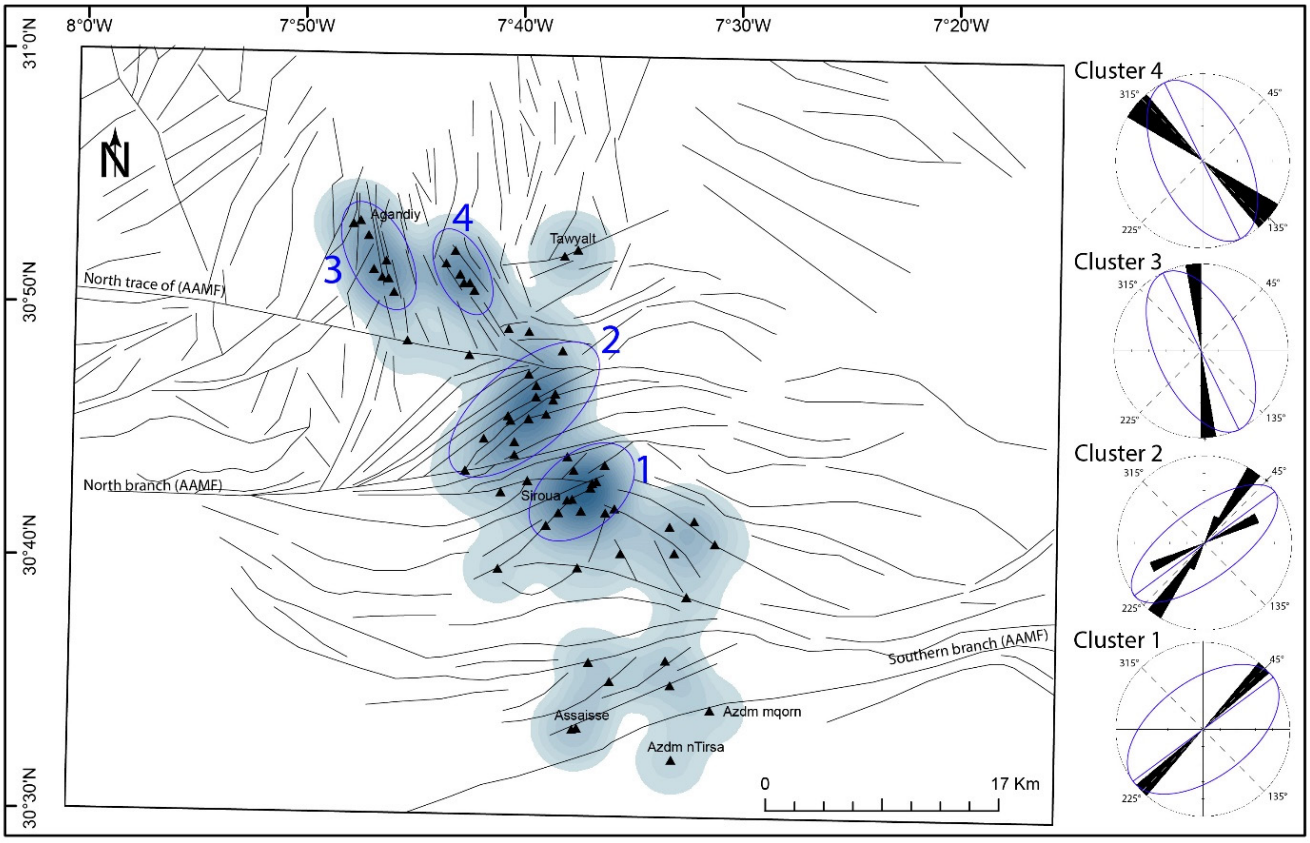

Figure 8: Vent density distribution map from Figure 5 with overlaid volcanic edifices (black triangles), mapped and inferred faults. Agglomerative hierarchical clustering reveals four clusters (blue ellipses). In the center of the Siroua volcanic field, Clusters 1 and 2 align NE–SW, while in the Agandiy region, Clusters 3 and 4 align NNW–SSE. The area south of Cluster 1 exhibits lower vent densities and a more dispersed distribution. On the right, rose diagrams compare the orientations of faults with the major axes of the ellipses for each cluster.

This aspect, combined with the structural influences from the southern Anti-Atlas ridge (Figure 1), which shows only a very limited amount of late Miocene deformation as documented by several authors [e.g. Sébrier et al. 2006; Malusà et al. 2007], suggests a complex interplay of geological factors shaping the volcanic landscape.

6.4 Factors influencing the evolution of the Siroua Volcanic Field

The Siroua volcanic field is an example of monogenetic volcanism developed in the complex setting of the Atlas mountains where coeval (since the late Miocene) mantle dynamics, volcanism, and crustal deformation contribute to its final evolution.

i. Mantle Dynamics: Several studies indicate that local isostasy cannot explain the high topography of the Moroccan Atlas. Although the exact process is still unclear, the uplift has been proposed to be driven by mantle upwellings due to the Canary plume [Missenard et al. 2006; Duggen et al. 2009; Civiero et al. 2018], lithospheric thinning [Ramdani 1998], or a combination of both [Zeyen et al. 2005; Duggen et al. 2009; Missenard and Cadoux 2011]. In addition, Lanari et al. [2023a] showed that the residual topography peaks precisely beneath the Siroua volcanic field, suggesting a potential link between volcanism and mantle dynamics.

ii. Volcanism: The anorogenic signature in the magmatism of the Siroua volcanic field indicates a deep mantle source for the volcanic activity in the region [see Lanari et al. 2023a, and references therein].

iii. Crustal Deformation: The Siroua volcanic field volcanism started during the middle Miocene [Berrahma and Delaloye 1989; Lanari et al. 2023a] together with a main deformation and cooling event as evidenced by low-temperature thermochronology [e.g. Leprêtre et al. 2018; Lanari et al. 2020a; b]. This contemporaneity is also confirmed by late Miocene Anti-Atlas volcanic deposits offset by oblique faults [Lanari et al. 2020a], suggesting a positive correlation between crustal deformation and magma ascent [e.g. Lanari et al. 2023b]. Tectonic structures (i.e. mapped pre-existing faults and inferred local structures) together with the regional and local stress state play a critical role in the spatial distribution of other volcanic edifices [e.g. Le Corvec et al. 2013b; Németh and Kereszturi 2015].

Our findings reveal that crustal faults oriented NE–SW and ENE–WSW, related to the pre-existing crustal Anti-Atlas

Major fault system, may favor the development of different magma pathways. Specifically, in the northern part of the Siroua volcanic field, the preferred alignment of volcanic edifices can be explained by the influence of shallow fractures and faults possibly related to local deformation. Local fractures and the local stress field could have generated preferential paths into discontinuities favoring magma ascent [e.g. Galland et al. 2007; Menand et al. 2010; Tibaldi et al. 2017].

7 Conclusions

i. We studied the Siroua volcanic field by combining statistical analyses on both the spatial distributions of volcanic edifices and their alignments, together with aeromagnetism and geological information. This approach provides an improved understanding of the volcanic activity of Siroua monogenetic volcanism.

ii. Spatial and density analysis allows the detection of clustering features that may not be apparent on visual observation. This may identify preferential areas for magma sources at depth.

iii. Aeromagnetism, as a geophysical imaging method, helps to identify masked faults underlying the massif of Siroua.

iv. Our analysis using Kernel Density Estimation indicates a deviation from a random Poisson distribution, highlighting elliptical biases aligned parallel to local fault systems. This pattern suggests that while volcanic edifices are not strictly aligned with tectonic structures, local structural controls and stress fields influence magma ascent directions.

v. Finally, our work confirms and documents a positive correlation between crustal deformation and the Siroua volcanic field's monogenetic centers. It must be emphasized that more detailed volcanological and structural studies of the field combined with new, more detailed radiometric ages are needed in the area to improve knowledge about the still debated spatio-temporal evolution of volcanic activity.

Author Contributions

MB: proposed the primary research idea. MB and AM: compiled, processed, and interpreted the aeromagnetic data. NL: processed, analyzed, and interpreted the statistical data. RL: provided key information and contributed valuable discussions on the geological context. All authors contributed to writing, reviewing, and editing the manuscript.

Acknowledgements

We are grateful to the "Direction de Géologie, Ministère de la Transition énergétique et du Développement durable" of Morocco (www.mem.gov.ma) for permission to use their aeromagnetic data for this study and the use of ARCMAP® software and OASIS montaj software™ for data processing. Thanks to Mhamed Berrahma for its constructive explanations during amazing field trip in the volcanic field of Siroua. We thank Francesco Mazzarini and reviewers for their constructive criticism and suggestions that has helped us to improve the final version of this paper.

Data Availability

The data that support the findings of this study are available from the corresponding author upon reasonable request.

Copyright notice

References

Agustín-Flores, J., C. Siebe, and M.-N. Guilbaud (2011). "Geology and geochemistry of Pelagatos, Cerro del Agua, and Dos Cerros monogenetic volcanoes in the Sierra Chichinautzin Volcanic Field, south of México City". *Journal of Volcanology and Geothermal Research* 201(1–4), pages 143–162. DOI: 10.1016/j.jvolgeores.2010.08.010.

Ait Brahim, L., P. Chotin, S. Hinaj, A. Abdelouafi, A. El Adraoui, C. Nakcha, D. Dhont, M. Charroud, F. Sossey Alaoui, M. Amrhar, A. Bouaza, H. Tabyaoui, and A. Chaouni (2002). "Paleostress evolution in the Moroccan African margin from Triassic to Present". *Tectonophysics* 357(1–4), pages 187–205. DOI: 10.1016/s0040-1951(02)00368-2.

Aït Hssaine, A. and D. Bridgland (2009). "Pliocene–Quaternary fluvial and aeolian records in the Souss Basin, southwest Morocco: A geomorphological model". *Global and Planetary Change* 68(4), pages 288–296. DOI: 10.1016/j.gloplacha.2009.03.002.

Amine, A., I.-E. El Amrani El Hassani, T. Remmal, F. El Kamel, B. Van Wyk De Vries, and P. Boivin (2019). "Geomorphological Classification and Landforms Inventory of the Middle-Atlas Volcanic Province (Morocco): Scientific Value and Educational Potential". *Quaestiones Geographicae* 38(1), pages 107–129. DOI: 10.2478/quageo-2019-0010.

Arboleya, M.-L., J. Babault, L. A. Owen, A. Teixell, and R. C. Finkel (2008). "Timing and nature of Quaternary fluvial incision in the Ouarzazate foreland basin, Morocco". *Journal of the Geological Society* 165(6), pages 1059–1073. DOI: 10.1144/0016-76492007-151.

Austin-Erickson, A., M. H. Ort, and G. Carrasco-Núñez (2011). "Rhyolitic phreatomagmatism explored: Tepexitl tuff ring (Eastern Mexican Volcanic Belt)". *Journal of Volcanology and Geothermal Research* 201(1–4), pages 325–341. DOI: 10.1016/j.jvolgeores.2010.09.007.

Baloga, S. M., L. S. Glaze, and B. C. Bruno (2007). "Nearest-neighbor analysis of small features on Mars: Applications to tumuli and rootless cones". *Journal of Geophysical Research: Planets* 112(E3). DOI: 10.1029/2005je002652.

Baranov, V. (1957). "A new method for interpretation of aeromagnetic maps: pseudo-gravimetric anomalies". *Geophysics* 22(2), pages 359–382. DOI: 10.1190/1.1438369.

Baranov, V. and H. Naudy (1964). "Numerical calculation of the formula of reduction to the magnetic pole". *Geophysics* 29(1), pages 67–79. DOI: 10.1190/1.1439334.

Bartolini, S., A. Cappello, J. Martí, and C. Del Negro (2013). "QVAST: a new Quantum GIS plugin for estimating volcanic susceptibility". *Natural Hazards and Earth System Sciences* 13(11), pages 3031–3042. DOI: 10.5194/nhess-13-3031-2013.

Bebbington, M. S. and S. J. Cronin (2011). "Spatio-temporal hazard estimation in the Auckland Volcanic Field, New Zealand, with a new event-order model". *Bulletin of Volcanology* 73(1), pages 55–72. DOI: 10.1007/s00445-010-0403-6.

Beggan, C. and C. W. Hamilton (2010). "New image processing software for analyzing object size-frequency distributions, geometry, orientation, and spatial distribution". *Computers & Geosciences* 36(4), pages 539–549. DOI: 10.1016/j.cageo.2009.09.003.

Bellon, H. (1976). *Séries magmatiques néogènes et quaternaires du pourtour de la Méditerranée occidentale, comparées dans leur cadre géochronométrique. Implications géodynamiques*. [Habilitation à diriger des recherches].

Benamrane, M., J. Francisco Santos, J. Mata, E. H. Talbi, M. Helena Mendes, L. Portela, S. Ribeiro, and M. Jadid (2023). "The alkaline intraplate Pliocene-Quaternary lavas from the Middle Atlas Volcanic Field (Morocco): Petrology, mineralogy and geochemistry". *Journal of African Earth Sciences* 205, page 105014. DOI: 10.1016/j.jafrearsci.2023.105014.

Benamrane, M., K. Németh, M. Jadid, and E. H. Talbi (2022). "Geomorphological Classification of Monogenetic Volcanoes and Its Implication to Tectonic Stress Orientation in the Middle Atlas Volcanic Field (Morocco)". *Land* 11(11), page 1893. DOI: 10.3390/land11111893.

Berrahma, M. (1982). "Le volcanisme mio-pliocène de la partie nord-ouest du Siroua (Anti-Atlas Central, Maroc): étude structurale et pétrographique". PhD thesis. Thèse de troisième cycle, Université Paris XI, France.

– (1995). *Etudes pétrologiques des laves récentes du massif du Siroua (Anti-Atlas, Maroc)*. Éd. du Service Géologique du Maroc.

Berrahma, M. and M. Delaloye (1989). "Données géochronologiques nouvelles sur le massif volcanique du Siroua (Anti-Atlas, maroc)". *Journal of African Earth Sciences (and the Middle East)* 9(3–4), pages 651–656. DOI: 10.1016/0899-5362(89)90049-3.

Berrahma, M., M. Delaloye, A. Faure-Muret, and H. Rachdi (1993). "Premières données géochronologiques sur le volcanisme alcalin du Jbel Saghro, Anti-Atlas, Maroc". *Journal of African Earth Sciences (and the Middle East)* 17(3), pages 333–341. DOI: 10.1016/0899-5362(93)90077-4.

Blaikie, T., L. Ailleres, P. Betts, and R. Cas (2014). "A geophysical comparison of the diatremes of simple and complex maar volcanoes, Newer Volcanics Province, south-eastern Australia". *Journal of Volcanology and Geothermal Research* 276, pages 64–81. DOI: 10.1016/j.jvolgeores.2014.03.001.

Blakely, R. J. (1995). *Potential Theory in Gravity and Magnetic Applications*. Cambridge University Press. ISBN: 9780511549816. DOI: 10.1017/cbo9780511549816.

Blakely, R. J. and R. W. Simpson (1986). "Approximating edges of source bodies from magnetic or gravity anomalies". *GEOPHYSICS* 51(7), pages 1494–1498. DOI: 10.1190/1.1442197.

Boulton, S., M. Stokes, and A. Mather (2014). "Transient fluvial incision as an indicator of active faulting and Plio-Quaternary uplift of the Moroccan High Atlas". *Tectonophysics* 633, pages 16–33. DOI: 10.1016/j.tecto.2014.06.032.

Boyce, J. (2013). "The Newer Volcanics Province of southeastern Australia: a new classification scheme and distribution map for eruption centres". *Australian Journal of Earth Sciences* 60(4), pages 449–462. DOI: 10.1080/08120099.2013.806954.

Cañón-Tapia, E. (2016). "Reappraisal of the significance of volcanic fields". *Journal of Volcanology and Geothermal Research* 310, pages 26–38. DOI: 10.1016/j.jvolgeores.2015.11.010.

– (2022). "Kernel Analyses of Volcanic Vent Distribution: How Accurate and Complete are the Objective Bandwidth Selectors?" *Frontiers in Earth Science* 10. DOI: 10.3389/feart.2022.779095.

Cas, R. A. F., J. van Otterloo, T. N. Blaikie, and J. van den Hove (2016). "The dynamics of a very large intraplate continental basaltic volcanic province, the Newer Volcanics Province, SE Australia, and implications for other provinces". *Geological Society, London, Special Publications* 446(1), pages 123–172. DOI: 10.1144/sp446.8.

Casalini, M., S. Tommasini, L. Guarnieri, R. Avanzinelli, M. Mattei, and S. Conticelli (2022). "Subduction-related lamproitic signature in intraplate-like volcanic rocks: the case study of the Tallante alkali basalts, Betic Chain, South-Eastern Spain". *Italian Journal of Geosciences* 141(1), pages 144–159. DOI: 10.3301/ijg.2022.06.

Cebriá, J., C. Martín-Escorza, J. López-Ruiz, D. Morán-Zenteno, and B. Martiny (2011). "Numerical recognition of alignments in monogenetic volcanic areas: Examples from the Michoacán-Guanajuato Volcanic Field in Mexico and Calatrava in Spain". *Journal of Volcanology and Geothermal Research* 201(1–4), pages 73–82. DOI: 10.1016/j.jvolgeores.2010.07.016.

Choubert, G. (1947). "L'accident majeur de l'Anti-Atlas". *Comptes Rendus de l'Academie des Sciences, Paris* 224, pages 1172–1173.

Choubert, G., R. Charlot, A. Faure-Muret, L. Hottinger, J. Marcais, D. Tisserant, and P. Vidal (1968). "Note préliminaire sur le volcanisme messinien-(pontien) au Maroc". *Comptes Rendus de l'Academie des Sciences, Paris* 266(série D), pages 197–199.

Civiero, C., V. Strak, S. Custódio, G. Silveira, N. Rawlinson, P. Arroucau, and C. Corela (2018). "A common deep source for upper-mantle upwellings below the Ibero-western Maghreb region from teleseismic P-wave traveltime tomography". *Earth and Planetary Science Letters* 499, pages 157–172. DOI: 10.1016/j.epsl.2018.07.024.

Clark, P. J. and F. C. Evans (1954). "Distance to Nearest Neighbor as a Measure of Spatial Relationships in Populations". *Ecology* 35(4), pages 445–453. DOI: 10.2307/1931034.

Clementucci, R., P. Ballato, L. L. Siame, C. Faccenna, S. Racano, G. Torreti, R. Lanari, L. Léanni, and V. Guillou (2023a). "Transient response to changes in uplift rates in the northern Atlas-Meseta system (Morocco)". *Geomorphology* 436, page 108765. DOI: 10.1016/j.geomorph.2023.108765.

Clementucci, R., P. Ballato, L. L. Siame, M. Fox, R. Lanari, A. Sembroni, C. Faccenna, A. Yaaqoub, and A. Essaifi (2023b). "Surface Uplift and Topographic Rejuvenation of a Tectonically Inactive Range: Insights From the Anti-Atlas and the Siroua Massif (Morocco)". *Tectonics* 42(2). DOI: 10.1029/2022tc007383.

Condit, C. D. and C. B. Connor (1996). *Geological Society of America Bulletin* 108(10), page 1225. DOI: 10.1130/0016-7606(1996)108<1225:rrovib>2.3.co;2.

Connor, C. B. (1987). "Structure of the Michoacán-Guanajuato volcanic field, Mexico". *Journal of Volcanology and Geothermal Research* 33(1–3), pages 191–200. DOI: 10.1016/0377-0273(87)90061-8.

Connor, C. B. and L. J. Connor (2009). "Estimating spatial density with kernel methods". *Volcanic and Tectonic Hazard Assessment for Nuclear Facilities*. Cambridge University Press, pages 346–368. ISBN: 9780511635380. DOI: 10.1017/cbo9780511635380.015.

Connor, C. B. and B. E. Hill (1995). "Three nonhomogeneous Poisson models for the probability of basaltic volcanism: Application to the Yucca Mountain region, Nevada". *Journal of Geophysical Research: Solid Earth* 100(B6), pages 10107–10125. DOI: 10.1029/95jb01055.

Connor, C. B., J. A. Stamatakos, D. A. Ferrill, B. E. Hill, G. I. Ofoegbu, F. M. Conway, B. Sagar, and J. Trapp (2000). "Geologic factors controlling patterns of small-volume basaltic volcanism: Application to a volcanic hazards assessment at Yucca Mountain, Nevada". *Journal of Geophysical Research: Solid Earth* 105(B1), pages 417–432. DOI: 10.1029/1999jb900353.

Cordell, L. and V. J. S. Grauch (1985). "Mapping Basement Magnetization Zones from Aeromagnetic Data in the San Juan Basin, New Mexico". *The Utility of Regional Gravity and Magnetic Anomaly Maps*. Society of Exploration Geophysicists, pages 181–197. ISBN: 9781560802723. DOI: 10.1190/1.0931830346.ch16.

Duggen, S., K. Hoernle, F. Hauff, A. Klügel, M. Bouabdellah, and M. Thirlwall (2009). "Flow of Canary mantle plume material through a subcontinental lithospheric corridor beneath Africa to the Mediterranean". *Geology* 37(3), pages 283–286. DOI: 10.1130/g25426a.1.

El Azzouzi, M., J. Bernard-Griffiths, H. Bellon, R. C. Maury, A. Piqué, S. Fourcade, J. Cotten, and J. Hernandez (1999). "Évolution des sources du volcanisme marocain au cours du Néogène". *Comptes Rendus de l'Académie des Sciences - Series IIA - Earth and Planetary Science* 329(2), pages 95–102. DOI: 10.1016/s1251-8050(99)80210-9.

El Bakkali, S. (1995). "Volcanologie et magmatologie du système du Gourougou (Rif oriental, Maroc)". PhD thesis. Clermont-Ferrand.

El Bakkali, S., A. Gourgaud, J.-L. Bourdier, H. Bellon, and N. Gundogdu (1998). "Post-collision neogene volcanism of the Eastern Rif (Morocco): magmatic evolution through time". *Lithos* 45(1–4), pages 523–543. DOI: 10.1016/s0024-4937(98)00048-6.

Emran, A. and F. Medina (2016). "Signification Des Structures N-S Du Plateau Des Aït Maghlif (Region D'eçundefinedour, Versant Meridional Du Massif Ancien Du Haut Atlas, Maroc)". *European Scientific Journal, ESJ* 12(15), page 365. DOI: 10.19044/esj.2016.v12n15p365.

Ennih, N. and J.-P. Liégeois (2001). "The Moroccan Anti-Atlas: the West African craton passive margin with limited Pan-African activity. Implications for the northern limit of the craton". *Precambrian Research* 112(3–4), pages 289–302. DOI: 10.1016/s0301-9268(01)00195-4.

Evjen, H. M. (1936). "The place of the vertical gradient in gravitational interpretations". *Geophysics* 1(1), pages 127–136. DOI: 10.1190/1.1437067.

Fairhead, J. D., A. Salem, L. Cascone, M. Hammill, S. Masterton, and E. Samson (2011). "New developments of the magnetic tilt-depth method to improve structural mapping of sedimentary basins". *Geophysical Prospecting* 59(6), pages 1072–1086. DOI: 10.1111/j.1365-2478.2011.01001.x.

Finn, C. A. and L. A. Morgan (2002). "High-resolution aeromagnetic mapping of volcanic terrain, Yellowstone National Park". *Journal of Volcanology and Geothermal Research* 115(1–2), pages 207–231. DOI: 10.1016/s0377-0273(01)00317-1.

Frizon de Lamotte, D., P. Leturmy, Y. Missenard, S. Khomsi, G. Ruiz, O. Saddiqi, F. Guillocheau, and A. Michard (2009). "Mesozoic and Cenozoic vertical movements in the Atlas system (Algeria, Morocco, Tunisia): An overview". *Tectonophysics* 475(1), pages 9–28. DOI: 10.1016/j.tecto.2008.10.024.

Frizon de Lamotte, D., B. Saint Bezar, R. Bracène, and E. Mercier (2000). "The two main steps of the Atlas building and geodynamics of the western Mediterranean". *Tectonics* 19(4), pages 740–761. DOI: 10.1029/2000tc900003.

Galland, O., E. Hallot, P. R. Cobbold, G. Ruffet, and J. de Bremond d'Ars (2007). "Volcanism in a compressional Andean setting: A structural and geochronological study of Tromen volcano (Neuquén province, Argentina)". *Tectonics* 26(4). DOI: 10.1029/2006tc002011.

Grauch, V. J. S. (2001). "Using high-resolution aeromagnetic surveys to map subsurface hydrogeology in sediment-filled basins: A case study over the Rio Grande rift, central New Mexico, USA". *ASEG Extended Abstracts* 2001(1), pages 1–4. DOI: 10.1071/aseg2001ab049.

Grauch, V. J. S. and M. R. Hudson (2007). "Guides to understanding the aeromagnetic expression of faults in sedimentary basins: Lessons learned from the central Rio Grande rift, New Mexico". *Geosphere* 3(6), page 596. DOI: 10.1130/ges00128.1.

Grauch, V. J. S., M. R. Hudson, S. A. Minor, and J. S. Caine (2006). "Sources of along-strike variation in magnetic anomalies related to intrasedimentary faults: A case study from the Rio Grande Rift, USA". *Exploration Geophysics* 37(4), pages 372–378. DOI: 10.1071/eg06372.

Guimerà, J., M. L. Arboleya, and A. Teixell (2011). "Structural control on present-day topography of a basement massif: the Central and Eastern Anti-Atlas (Morocco)". *Geologica Acta: an international earth science journal* 9(1), pages 55–65. DOI: 10.1344/105.000001643.

Hamilton, C. W., S. A. Fagents, and T. Thordarson (2010). "Explosive lava–water interactions II: self-organization processes among volcanic rootless eruption sites in the 1783–1784 Laki lava flow, Iceland". *Bulletin of Volcanology* 72(4), pages 469–485. DOI: 10.1007/s00445-009-0331-5.

Harmand, C. and J. Cantagrel (1984). "Le volcanisme alcalin tertiaire et quaternaire du moyen atlas (Maroc): chronologie K/Ar et cadre géodynamique". *Journal of African Earth Sciences (1983)* 2(1), pages 51–55. DOI: 10.1016/0899-5362(84)90019-8.

Hernandez, J. and H. Bellon (1985). "Chronologie K-Ar du volcanisme miocène du Rif oriental (Maroc): implications tectoniques et magmatologiques". *Revue de géologie dynamique et de géographie physique* 26(2), pages 85–94.

Hodel, F., A. Triantafyllou, J. Berger, M. Macouin, J.-M. Baele, N. Mattielli, C. Monnier, R. Trindade, M. Ducea, A. Chatir, N. Ennih, J. Langlade, and M. Poujol (2020). "The Moroccan Anti-Atlas ophiolites: Timing and melting processes in an intra-oceanic arc-back-arc environment". *Gondwana Research* 86, pages 182–202. DOI: 10.1016/j.gr.2020.05.014.

Holcombe, R. (2010). *GEOrient, v. 9.4.0*. Software. URL: https://www.holcombe.net.au/software/georient.html (visited on 10/01/2024).

Isles, D. J. and L. R. Rankin (2013). *Geological interpretation of aeromagnetic data*. Society of Exploration Geophysicists and Australian Society of Exploration Geophysicists. ISBN: 9781560803218. DOI: 10.1190/1.9781560803218.ref.

Jordan, S. C., R. A. F. Cas, and P. C. Hayman (2013). "The origin of a large (<3km) maar volcano by coalescence of multiple shallow craters: Lake Purrumbete maar, southeastern Australia". *Journal of Volcanology and Geothermal Research* 254, pages 5–22. DOI: 10.1016/j.jvolgeores.2012.12.019.

Kiyosugi, K., C. B. Connor, P. H. Wetmore, B. P. Ferwerda, A. M. Germa, L. J. Connor, and A. R. Hintz (2012). "Relationship between dike and volcanic conduit distribution in a highly eroded monogenetic volcanic field: San Rafael, Utah, USA". *Geology* 40(8), pages 695–698. DOI: 10.1130/g33074.1.

Lahti, I. and T. Karinen (2010). "Tilt derivative multiscale edges of magnetic data". *The Leading Edge* 29(1), pages 24–29. DOI: 10.1190/1.3284049.

Lanari, R., A. Boutoux, C. Faccenna, F. Herman, S. D. Willett, and P. Ballato (2023a). "Cenozoic exhumation in the Mediterranean and the Middle East". *Earth-Science Reviews* 237, page 104328. DOI: 10.1016/j.earscirev.2023.104328.

Lanari, R., C. Faccenna, M. G. Fellin, A. Essaifi, A. Nahid, F. Medina, and N. Youbi (2020a). "Tectonic Evolution of the Western High Atlas of Morocco: Oblique Convergence, Reactivation, and Transpression". *Tectonics* 39(3). DOI: 10.1029/2019tc005563.

Lanari, R., C. Faccenna, C. Natali, E. Şengül Uluocak, M. G. Fellin, T. W. Becker, O. H. Göğüş, N. Youbi, R. Clementucci, and S. Conticelli (2023b). "The Atlas of Morocco: A Plume-Assisted Orogeny". *Geochemistry, Geophysics, Geosystems* 24(6). DOI: 10.1029/2022gc010843.

Lanari, R., M. G. Fellin, C. Faccenna, M. L. Balestrieri, F. J. Pazzaglia, N. Youbi, and C. Maden (2020b). "Exhumation and Surface Evolution of the Western High Atlas and Surrounding Regions as Constrained by Low-Temperature Thermochronology". *Tectonics* 39(3). DOI: 10.1029/2019tc005562.

Lanari, R., R. Reitano, E. Giachetta, F. J. Pazzaglia, R. Clementucci, C. Faccenna, and M. G. Fellin (2022). "Is the Anti-Atlas of Morocco still uplifting?" *Journal of African Earth Sciences* 188, page 104481. DOI: 10.1016/j.jafrearsci.2022.104481.

Le Corvec, N., T. Menand, and J. Lindsay (2013a). "Interaction of ascending magma with pre-existing crustal fractures in monogenetic basaltic volcanism: an experimental approach". *Journal of Geophysical Research: Solid Earth* 118(3), pages 968–984. DOI: 10.1002/jgrb.50142.

Le Corvec, N., K. B. Spörli, J. Rowland, and J. Lindsay (2013b). "Spatial distribution and alignments of volcanic centers: Clues to the formation of monogenetic volcanic fields". *Earth-Science Reviews* 124, pages 96–114. DOI: 10.1016/j.earscirev.2013.05.005.

Leprêtre, R., Y. Missenard, J. Barbarand, C. Gautheron, I. Jouvie, and O. Saddiqi (2018). "Polyphased Inversions of an Intracontinental Rift: Case Study of the Marrakech High Atlas, Morocco". *Tectonics* 37(3), pages 818–841. DOI: 10.1002/2017tc004693.

Leprêtre, R., Y. Missenard, B. Saint-Bezar, J. Barbarand, G. Delpech, J. Yans, A. Dekoninck, and O. Saddiqi (2015). "The three main steps of the Marrakech High Atlas building in Morocco: Structural evidences from the southern foreland, Imini area". *Journal of African Earth Sciences* 109, pages 177–194. DOI: 10.1016/j.jafrearsci.2015.05.013.

Lesti, C., G. Giordano, F. Salvini, and R. Cas (2008). "Volcano tectonic setting of the intraplate, Pliocene-Holocene, Newer Volcanic Province (southeast Australia): Role of crustal fracture zones". *Journal of Geophysical Research: Solid Earth* 113(B7). DOI: 10.1029/2007jb005110.

Lutz, T. M. and J. T. Gutmann (1995). "An improved method for determining and characterizing alignments of point-like features and its implications for the Pinacate volcanic field, Sonora, Mexico". *Journal of Geophysical Research: Solid Earth* 100(B9), pages 17659–17670. DOI: 10.1029/95jb01058.

Malusà, M. G., R. Polino, A. C. Feroni, A. Ellero, G. Ottria, L. Baidder, and G. Musumeci (2007). "Post-Variscan tectonics in eastern Anti-Atlas (Morocco)". *Terra Nova* 19(6), pages 481–489. DOI: 10.1111/j.1365-3121.2007.00775.x.

Martin, A. J., K. Umeda, C. B. Connor, J. N. Weller, D. Zhao, and M. Takahashi (2004). "Modeling long-term volcanic hazards through Bayesian inference: An example from the Tohoku volcanic arc, Japan". *Journal of Geophysical Research: Solid Earth* 109(B10). DOI: 10.1029/2004jb003201.

Mattauer, M., F. Proust, and P. Tapponnier (1972). "Major Strike-slip Fault of Late Hercynian Age in Morocco". *Nature* 237(5351), pages 160–162. DOI: 10.1038/237160b0.

Mattauer, M., P. Tapponnier, and F. Proust (1977). "Sur les mecanismes de formation des chaines intracontinentales; l'exemple des chaines atlasiques du Maroc". *Bulletin de la Société géologique de France* 7(3), pages 521–526.

Mazzarini, F. (2003). "Spatial distribution of cones and satellite-detected lineaments in the Pali Aike Volcanic Field (southernmost Patagonia): insights into the tectonic setting of a Neogene rift system". *Journal of Volcanology and Geothermal Research* 125(3–4), pages 291–305. DOI: 10.1016/s0377-0273(03)00120-3.

– (2007). "Vent distribution and crustal thickness in stretched continental crust: The case of the Afar Depression (Ethiopia)". *Geosphere* 3(3), page 152. DOI: 10.1130/ges00070.1.

Mazzarini, F., L. Ferrari, and I. Isola (2010). "Self-similar clustering of cinder cones and crust thickness in the Michoacan–Guanajuato and Sierra de Chichinautzin volcanic fields, Trans-Mexican Volcanic Belt". *Tectonophysics* 486(1–4), pages 55–64. DOI: 10.1016/j.tecto.2010.02.009.

Mazzarini, F. and I. Isola (2021). "Vent distribution and structural inheritance in an embryonic rift: The example of the Chyulu Hills off-rift magmatic range (South Kenya)". *Journal of Volcanology and Geothermal Research* 416, page 107268. DOI: 10.1016/j.jvolgeores.2021.107268.

Meghraoui, M., F. Outtani, A. Choukri, and D. Frizon de Lamotte (1999). "Coastal Tectonics across the South Atlas Thrust Front and the Agadir Active Zone, Morocco". *Geological Society, London, Special Publications* 146(1), pages 239–253. DOI: 10.1144/gsl.sp.1999.146.01.14.

Menand, T., K. A. Daniels, and P. Benghiat (2010). "Dyke propagation and sill formation in a compressive tectonic environment". *Journal of Geophysical Research: Solid Earth* 115(B8). DOI: 10.1029/2009jb006791.

Menzies, M., P. Kempton, and M. Dungan (1985). "Interaction of Continental Lithosphere and Asthenospheric Melts below the Geronimo Volcanic Field, Arizona, U.S.A". *Journal of Petrology* 26(3), pages 663–693. DOI: 10.1093/petrology/26.3.663.

Miller, H. G. and V. Singh (1994). "Potential field tilt—a new concept for location of potential field sources". *Journal of Applied Geophysics* 32(2–3), pages 213–217. DOI: 10.1016/0926-9851(94)90022-1.

Milligan, P. R. and P. J. Gunn (1997). "Enhancement and presentation of airborne geophysical data". *AGSO Journal of Australian Geology and Geophysics* 17(2), pages 63–75.

Missenard, Y. and A. Cadoux (2011). "Can Moroccan Atlas lithospheric thinning and volcanism be induced by Edge-Driven Convection?" *Terra Nova* 24(1), pages 27–33. DOI: 10.1111/j.1365-3121.2011.01033.x.

Missenard, Y., H. Zeyen, D. Frizon de Lamotte, P. Leturmy, C. Petit, M. Sébrier, and O. Saddiqi (2006). "Crustal versus asthenospheric origin of relief of the Atlas Mountains of Morocco". *Journal of Geophysical Research: Solid Earth* 111(B3). DOI: 10.1029/2005jb003708.

Morfulis, M., W. Báez, S. Retamoso, L. Bardelli, R. Filipovich, and C. A. Sommer (2020). "Quantitative spatial distribution analysis of mafic monogenic volcanism in the southern Puna, Argentina: Implications for magma production rates and structural control during its ascent". *Journal of South American Earth Sciences* 104, page 102852. DOI: 10.1016/j.jsames.2020.102852.

Moukadiri, A. and C. Pin (1998). "Géochimie / Geochemistry Géomatériaux / Geomaterials Géochimie (éléments majeurs et terres rares) des granulites méta-sédimentaires en xénolithes dans les basaltes alcalins quaternaires du Moyen Atlas (Maroc): Arguments en faveur de la nature pour partie restitique de la croûte inférieure". *Comptes Rendus de l'Académie des Sciences - Series IIA - Earth and Planetary Science* 327(9), pages 589–595. DOI: 10.1016/s1251-8050(99)80112-8.

Muirhead, J. D., S. A. Kattenhorn, H. Lee, S. Mana, B. D. Turrin, T. P. Fischer, G. Kianji, E. Dindi, and D. S. Stamps (2016a). "Evolution of upper crustal faulting assisted by magmatic volatile release during early-stage continental rift development in the East African Rift". *Geosphere* 12(6), pages 1670–1700. DOI: 10.1130/ges01375.1.

Muirhead, J. D., A. R. Van Eaton, G. Re, J. D. L. White, and M. H. Ort (2016b). "Monogenetic volcanoes fed by interconnected dikes and sills in the Hopi Buttes volcanic field, Navajo Nation, USA". *Bulletin of Volcanology* 78(2). DOI: 10.1007/s00445-016-1005-8.

Nabighian, M. N., V. J. S. Grauch, R. O. Hansen, T. R. LaFehr, Y. Li, J. W. Peirce, J. D. Phillips, and M. E. Ruder (2005). "The historical development of the magnetic method in exploration". *Geophysics* 70(6), 33ND–61ND. DOI: 10.1190/1.2133784.

Németh, K. and G. Kereszturi (2015). "Monogenetic volcanism: personal views and discussion". *International Journal of Earth Sciences* 104(8), pages 2131–2146. DOI: 10.1007/s00531-015-1243-6.

Németh, K. (2010). "Monogenetic volcanic fields: Origin, sedimentary record, and relationship with polygenetic volcanism". *What Is a Volcano?* Geological Society of America. ISBN: 9780813724706. DOI: 10.1130/2010.2470(04).

Pastor, A., J. Babault, L. A. Owen, A. Teixell, and M.-L. Arboleya (2015). "Extracting dynamic topography from river profiles and cosmogenic nuclide geochronology in the Middle Atlas and the High Plateaus of Morocco". *Tectonophysics* 663, pages 95–109. DOI: 10.1016/j.tecto.2015.06.007.

Proust, F., J.-P. Petit, and P. Tapponnier (1977). "L'accident du Tizi n'Test et le role des decrochements dans la tectonique du Haut Atlas occidental (Maroc)". *Bulletin de la Société Géologique de France* S7-XIX(3), pages 541–551. DOI: 10.2113/gssgfbull.s7-xix.3.541.

Rachdi, H. E.-N., D. Velde, and J. Hernández (1985). "L'association volcanique plio-quaternaire basanite-néphélinite-phonolite du Maroc central". *Comptes rendus de l'Académie des sciences. Série 2, Mécanique, Physique, Chimie, Sciences de l'univers, Sciences de la Terre* 301(18), pages 1293–1298.

Ramdani, F. (1998). "Geodynamic implications of intermediate-depth earthquakes and volcanism in the intraplate Atlas mountains (Morocco)". *Physics of the Earth and Planetary Interiors* 108(3), pages 245–260. DOI: 10.1016/s0031-9201(98)00106-x.

Rossi, M. J. (1996). "Morphology and mechanism of eruption of postglacial shield volcanoes in Iceland". *Bulletin of Volcanology* 57(7), pages 530–540. DOI: 10.1007/bf00304437.

Runge, M. G., M. S. Bebbington, S. J. Cronin, J. M. Lindsay, C. L. Kenedi, and M. R. H. Moufti (2014). "Vents to events: determining an eruption event record from volcanic vent structures for the Harrat Rahat, Saudi Arabia". *Bulletin of Volcanology* 76(3). DOI: 10.1007/s00445-014-0804-z.

Sébrier, M., L. Siame, E. M. Zouine, T. Winter, Y. Missenard, and P. Leturmy (2006). "Active tectonics in the Moroccan High Atlas". *Comptes Rendus. Géoscience* 338(1–2), pages 65–79. DOI: 10.1016/j.crte.2005.12.001.

Silverman, B. W. (1986). *Density estimation for statistics and data analysis*. 1st edition. Routledge. ISBN: 9780412246203.

Smith, I. E. M. and K. Németh (2017). "Source to surface model of monogenetic volcanism: a critical review". *Geological Society, London, Special Publications* 446(1), pages 1–28. DOI: 10.1144/sp446.14.

Soumaya, A., N. Ben Ayed, M. Rajabi, M. Meghraoui, D. Delvaux, A. Kadri, M. Ziegler, S. Maouche, and A. Braham (2018). "Active Faulting Geometry and Stress Pattern Near Complex Strike-Slip Systems Along the Maghreb Region: Constraints on Active Convergence in the Western Mediterranean". *Tectonics* 37(9), pages 3148–3173. DOI: 10.1029/2018tc004983.

Spörli, K. B. and V. R. Eastwood (1997). "Elliptical boundary of an intraplate volcanic field, Auckland, New Zealand". *Journal of Volcanology and Geothermal Research* 79(3–4), pages 169–179. DOI: 10.1016/s0377-0273(97)00030-9.

Tesón, E. and A. Teixell (2008). "Sequence of thrusting and syntectonic sedimentation in the eastern Sub-Atlas thrust belt (Dadès and Mgoun valleys, Morocco)". *International Journal of Earth Sciences* 97(1), pages 103–113. DOI: 10.1007/s00531-006-0151-1.

Tibaldi, A., F. L. Bonali, and C. Corazzato (2017). "Structural control on volcanoes and magma paths from local- to orogen-scale: The central Andes case". *Tectonophysics* 699, pages 16–41. DOI: 10.1016/j.tecto.2017.01.005.

Turner, S. P., J. P. Platt, R. M. M. George, S. P. Kelley, D. G. Pearson, and G. M. Nowell (1999). "Magmatism Associated with Orogenic Collapse of the Betic-Alboran Domain, SE Spain". *Journal of Petrology* 40(6), pages 1011–1036. DOI: 10.1093/petroj/40.6.1011.

Van Otterloo, J., M. Raveggi, R. A. F. Cas, and R. Maas (2014). "Polymagmatic Activity at the Monogenetic Mt Gambier Volcanic Complex in the Newer Volcanics Province, SE Australia: New Insights into the Occurrence of Intraplate Volcanic Activity in Australia". *Journal of Petrology* 55(7), pages 1317–1351. DOI: 10.1093/petrology/egu026.

Verduzco, B., J. D. Fairhead, C. M. Green, and C. MacKenzie (2004). "New insights into magnetic derivatives for structural mapping". *The Leading Edge* 23(2), pages 116–119. DOI: 10.1190/1.1651454.

Wand, M. P. and M. C. Jones (1994). *Kernel smoothing*. Chapman & Hall/CRC press. ISBN: 0-412-55270-1.

Zeyen, H., P. Ayarza, M. Fernàndez, and A. Rimi (2005). "Lithospheric structure under the western African-European plate boundary: A transect across the Atlas Mountains and the Gulf of Cadiz". *Tectonics* 24(2). DOI: 10.1029/2004tc001639.